Automatic Locating of Anthropometric Landmarks on 3D Human Models

Zouhour Ben Azouz and Chang Shu

National Research Council of Canada
Institute of Information Technology
Visual Information Technology Group

Anthropometry

Traditional Anthropometry

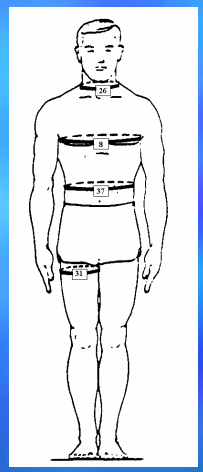

Poor description of the body shape

3D surface Anthropometry

Captures the details of the body Shape within a few seconds

3D Anthropometric Data

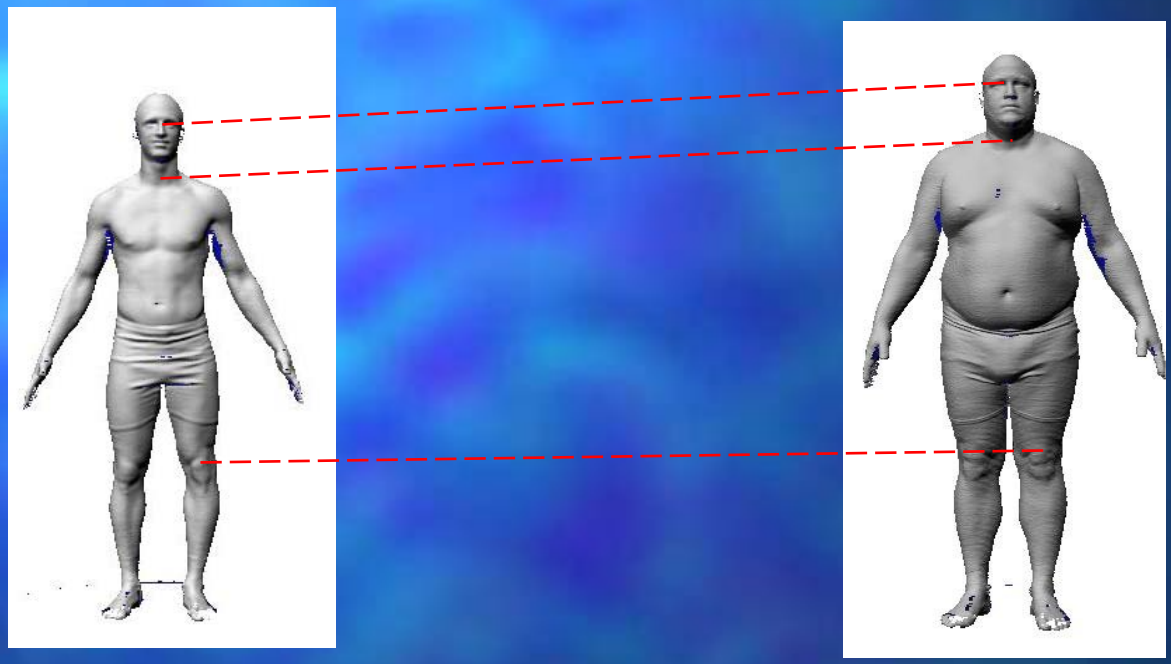

172 267 surface points

191 412 surface points

No correspondence

Establishing Correspondence between Human Scans

- Canonical sampling **(Tahan, Buxton, Ruiz, 2005)**
  - regularly sample each model
  - requires segmentation
- Volumetric method **(Ben Azouz, Shu, Lepage, Rioux, 2005)**
  - volumetric representation
  - signed distance
  - landmark free
- **Template fitting (Allen, Curless, and Popovic, 2003)**
  - **fit a template human model to instances of human scans**

Establishing Correspondence between Human Scans (cont)

Template fitting **(Allen, Curless, and Popovic, 2003)**

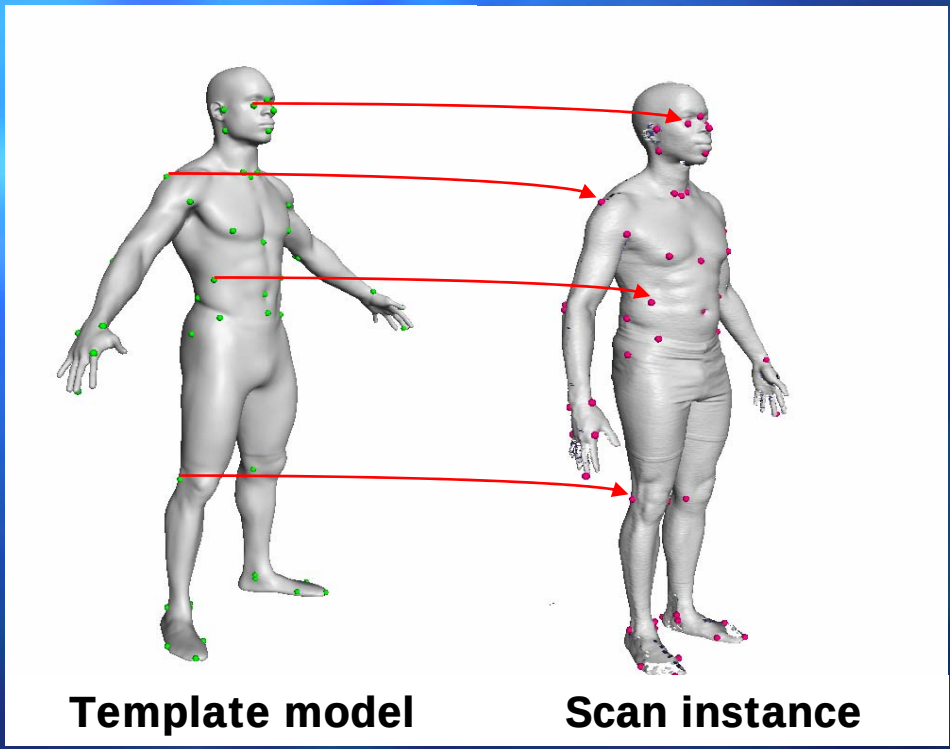

Requires anthropometric landmarks

Anthropometric Landmarks

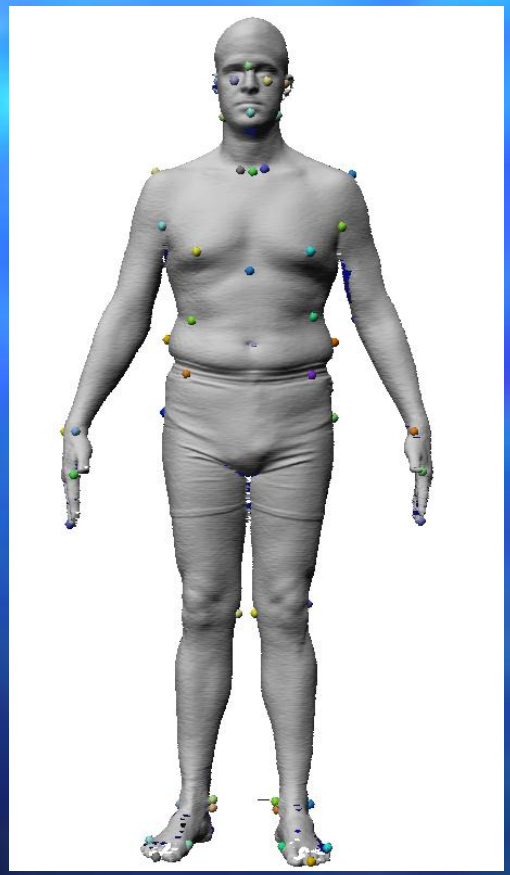

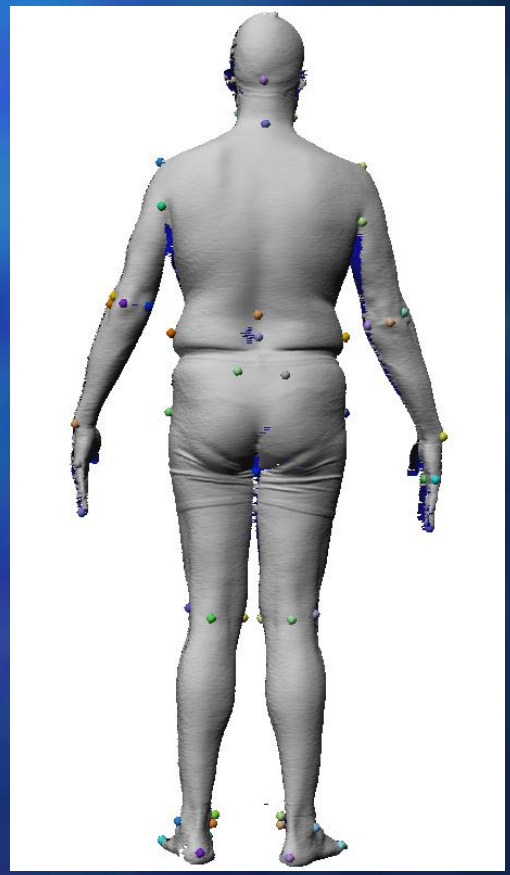

Previous work on Anthropometric Landmark locating

Landmark locating based on prior marking

- G.R. Geisen,C.P. Mason, ″Automatic Detection, Identification, and Registration of Anatomical Landmarks,″ 1995.

- D. Burnsides, M. Boehmer and K.M. Robinette, ″3-D Landmark Detection and Identification in the CAESAR Project,″ 2001.

Previous work on Anthropometric Landmarks locating (cont)

Landmark locating without prior marking

- A. Certain and W. Stueltzle, ″Automatic Body Measurement for Mass Customization of Garments,″ 1999.

- L. Dekker, I. Douros, B.F. Buxton and P. Treleaven, ″Building Symbolic Information for 3D Human Body Modeling from Range Data,″ 1999.

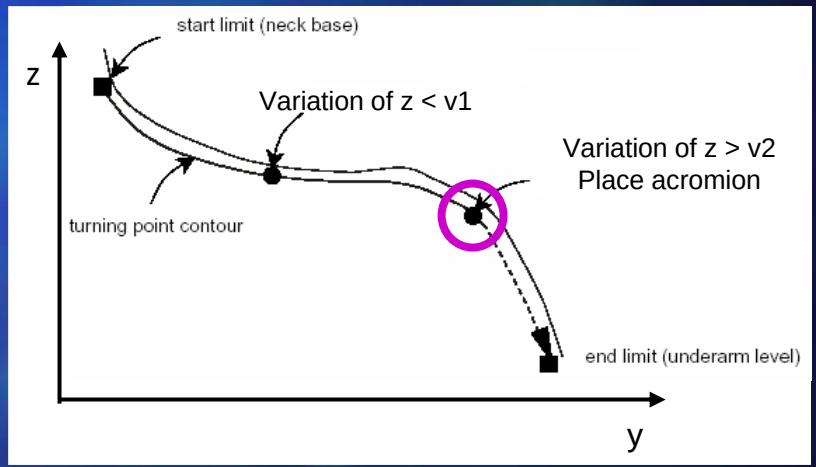

Objectifs

- Locating automatically landmarks based on learning techniques.
- Use a general framework to identify all the landmarks.

Landmark Locating problem

- Learning step:
  - Local surface properties of landmarks.
  - The spatial relationship between landmarks.

- Matching step: for an instance of a human model assign to the anthropometric landmarks the position that is the most compatible with the learned information.

Pairwise Markov Random Field (MRF)

$L = \{l_1, l_2, .., l_i, ...l_n\}$

l_i is the position of the landmark i

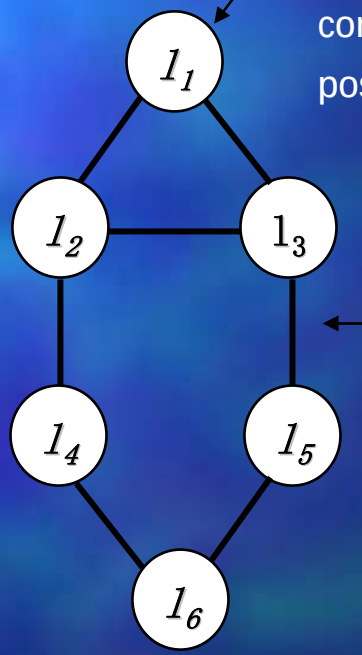

$\Phi_i(l_i)$

Likelihood that landmark l_i correspond to a given position on the surface

$\psi_{ij}(l_i, l_j)$

Compatibility between the Positions of landmark pairs

The joint probability represented by a pairwise MRF:

$$P(L) = \frac{1}{Z} \prod_i \Phi_i(l_i) \prod_{i,j} \Psi(l_i, l_j)$$

Landmark locating using a pairwise MRF

- Learning step: define the parameters of the probabilities associated to the MRF.
- Probabilistic inference step: Assign to each landmark the position that maximizes the joint probability defined by the MRF.

Learning step

Local surface properties

$\Phi_i(I_i)$ is a gaussian distribution of **Spin Images**

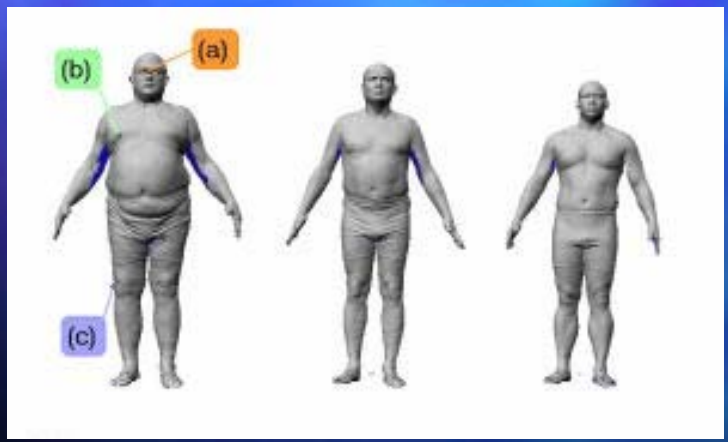

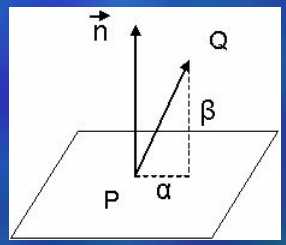

[Johnson 97]

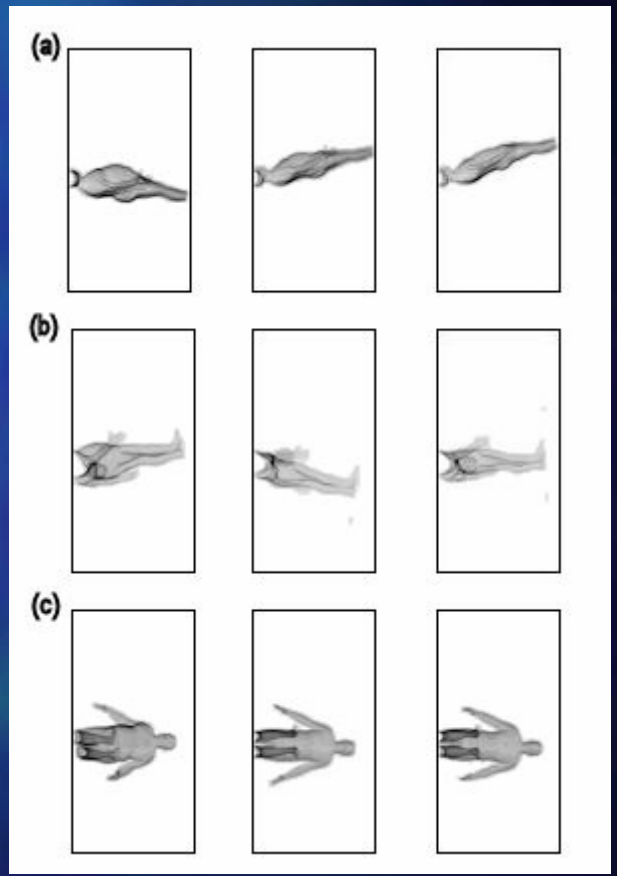

Learning step

Spatial relationship between landmarks

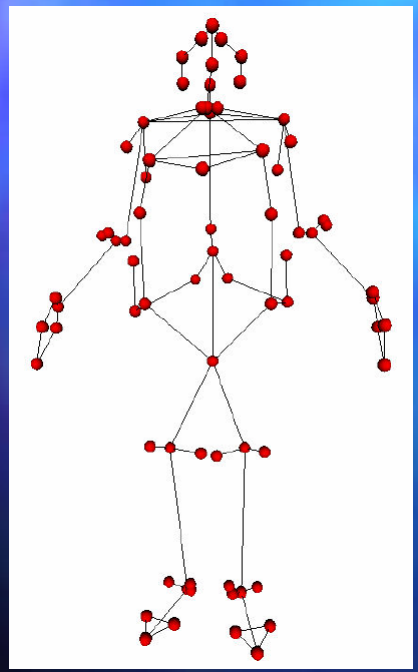

Structure of the landmark graph
(73 landmarks)

$\psi_{ij}(l_i, l_j)$ is a gaussian distribution of the relative position of landmark l_j with respect to landmark l_i.

Probabilistic Inference

Loopy Belief Propagation

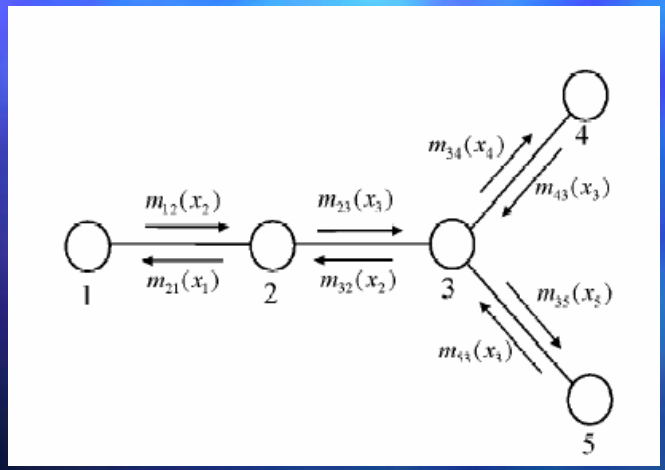

Maximizing the probability function:

$$P(L) = \frac{1}{Z}\prod_i \phi_i(l_i)\prod_{i,j}\psi_{ij}(l_i, l_j)$$

through message passing:

$$m_{ij}^{t+1}(l_j) = \sum_{l_i}\phi_i(l_i)\psi_{ij}(l_i, l_j)\prod_{k\in N(i)-\{j\}} m_{ki}^{t}(l_i)$$

$$b_i(l_i) = k\phi_i(l_i)\prod_{j\in N(i)} m_{ji}(l_i)$$

Attribute to each landmark the position that has the highest belief

Experimental Results

Training set of 200 human models from the CAESAR data base

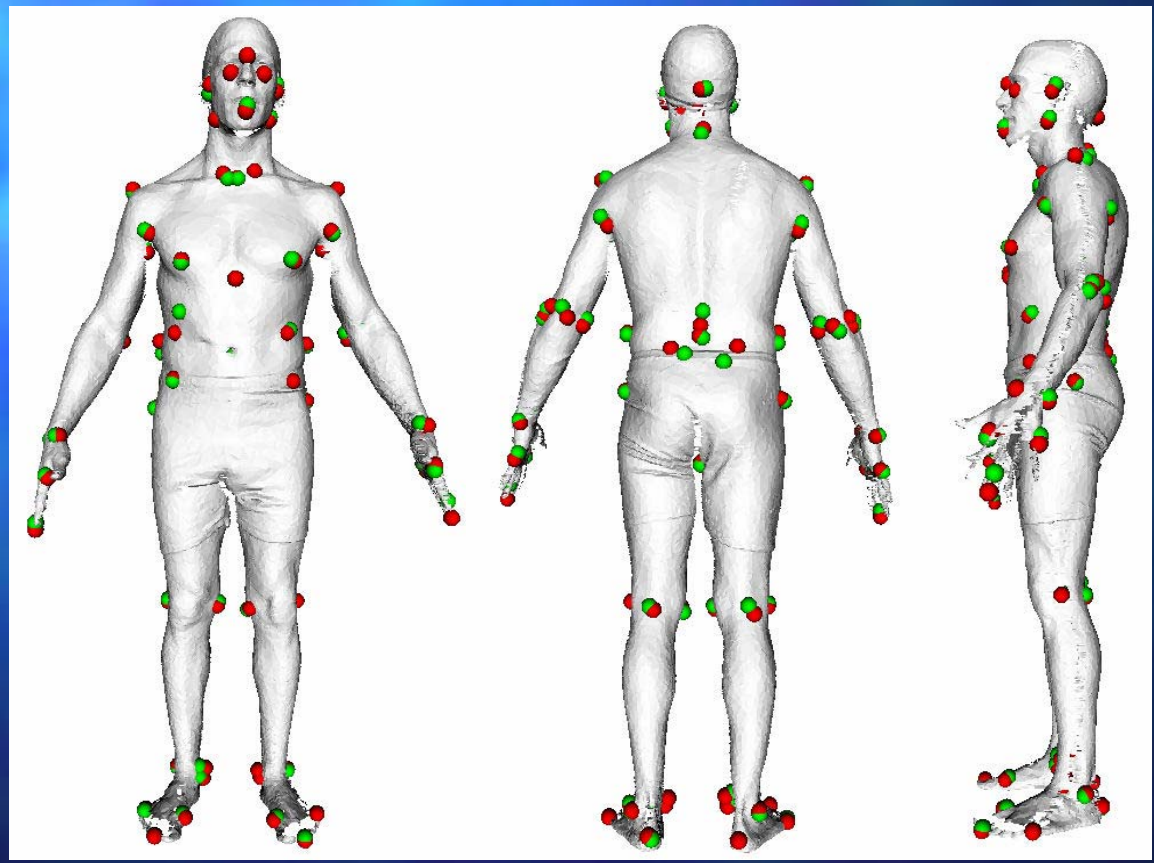

Experimental Results

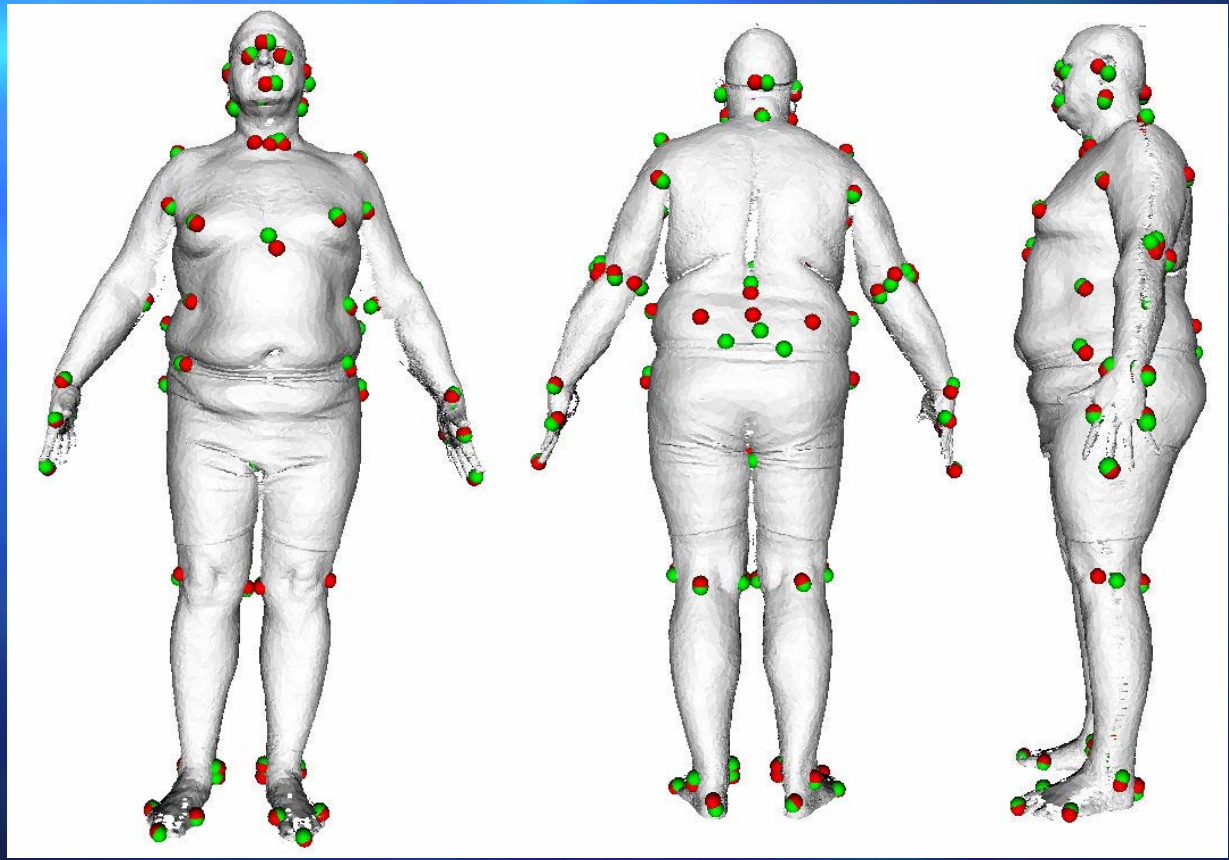

Experimental Results

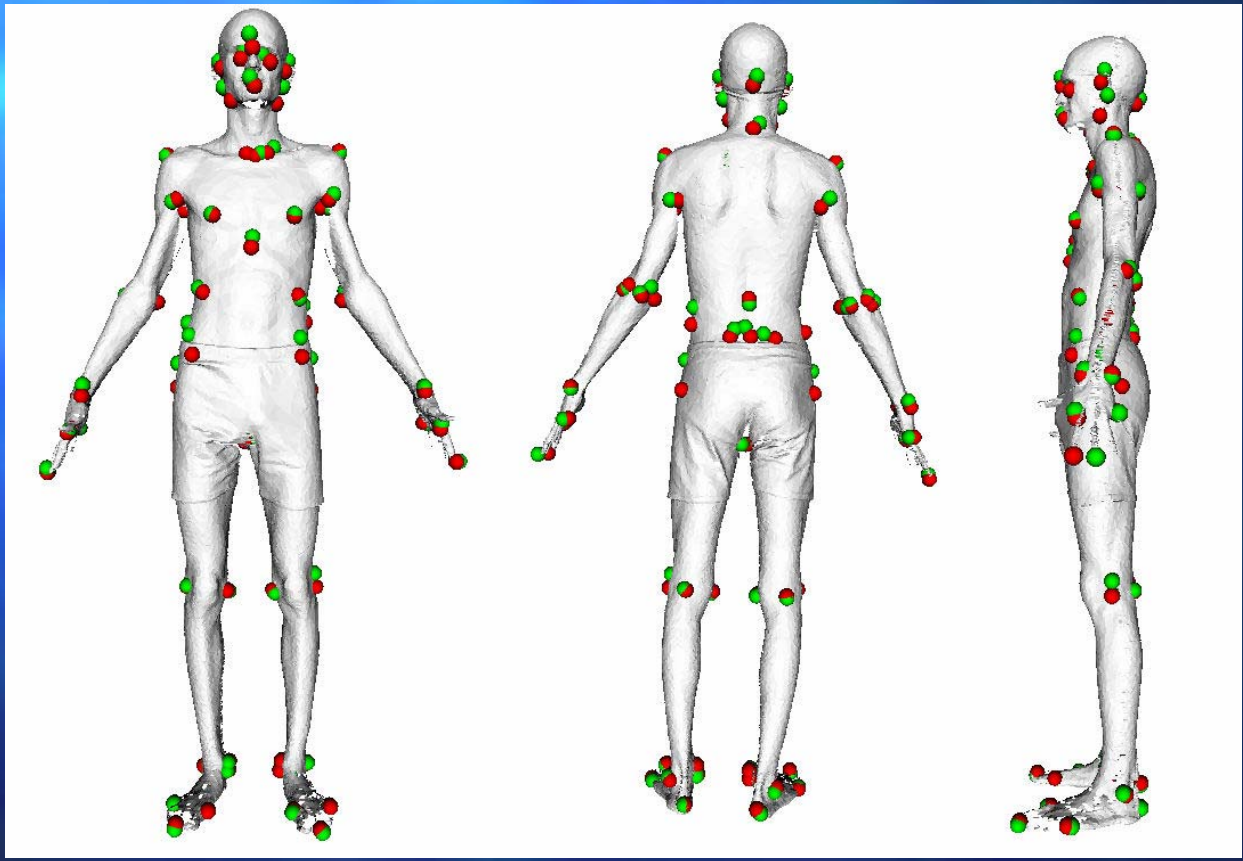

Experimental Results

Error of landmark locating computed over 30 test human models.

Landmark	Average (mm)	Landmark	Average (mm)
1 Sellion	10	38 Rt. Dactylion	12
2 Rt. Infraorbitale	7.1	39 Rt. Ulnar Styloid	11
3 Lt. Infraorbitale	11	40 Rt. Metacarpal-Phal. V	7.6
4 Supramenton	12	41 Lt. Acromion	12
5 Rt. Tragion	13	42 Lt. Axilla, Ant	13
6 Rt. Gonion	16	43 Lt. Radial Styloid	11
7 Lt. Tragion	16	44 Lt. Axilla, Post.	15
8 Lt. Gonion	15	45 Lt. Olecranon	13
9 Nuchale	20	46 Lt. Humeral Lateral Epicn	13
10 Rt. Clavicale	10	47 Lt. Humeral Medial Epicn	18
11 Suprasternale	12	48 Lt. Radiale	16
12 Lt. Clavicale	13	49 Lt. Metacarpal-Phal. II	7.6
13 Rt. Thelion/Bustpoint	4.8	50 Lt. Dactylion	9.5
14 Lt. Thelion/Bustpoint	7.2	51 Lt. Ulnar Styloid	27
15 Substernale	16	52 Lt. Metacarpal-Phal. V	8.9
16 Rt. 10th Rib	27	53 Rt. Knee Crease	11
17 Rt. ASIS	33	54 Rt. Femoral Lateral Epicn	14
18 Lt. 10th Rib	21	55 Rt. Femoral Medial Epicn	15
19 Lt. ASIS	27	56 Rt. Metatarsal-Phal. V	8
20 Rt. Iliocristale	17	57 Rt. Lateral Malleolus	12
21 Rt. Trochanterion	16	58 Rt. Medial Malleolus	12
22 Lt. Iliocristale	16	59 Rt. Sphyrion	9.3

Conclusion and Future work

- Our Approach locates a large number of anthropometric landmarks without placing markers on all the measured individuals witch is useful for future 3D anthropometric data collection.
- The current results can be improved by:
  - Identifying automatically the most correlated pairs of landmarks.
  - Developing surface descriptors that are posture and resolution invariant .
  - Use of geodesic distance to characterize the spatial relationship between pairs of landmarks.